Voyager Mission, Detailed processing of weak magnetic fields;
I - Constraints to the uncertainties of the calibrated magnetic field signal in the Voyager missions

by Daniel B. Berdichevsky 5/22/2009

a work possible only through the many suggestions/input form Mario H. Acuña, vers. 12/17/2008
suggestions by Leonard Burlaga, 12/30/2008 & 05/18/2009
title/suggestions by Norman Ness, 03/09/2009

1. Introduction

The main purpose of this study is to describe the tools, developed by the MAG team to provide the most reliable, magnetic field information possible from the 'Voyager' mission. This includes a brief review of:
a) The standard calibration method, which uses a few rotations per year of the three axes stabilized spacecraft around a fix rotation axis. The rotation axis is along the Z payload axis, a direction radial from the Sun to within less than 0.3º at ~ 60 AU or more from the Earth.
b) The in-space sensor calibration which uses a coil wound around the periphery of the high gain antenna of the spacecraft. When energized the coil produces – at the location of the sensors – a magnetic field whose direction and intensity is accurately known. Each rotation lasts ~20min.
c) The steps taken in the standard process of generating from the signal the calibrated magnetic field. (See appendix **Method**).
Also a new technique is introduced here. This technique uses the electronic calibration (MAGCAL) technique of the flux gate magnetometers in the voyager mission to help us constraint uncertainties regarding the value of the space plasma magnetic field intensity and orientation. Every 29 days a MAGCAL provides calibration when the phase of the high frequency signal in the sensor [the sensing coil and its nucleus (1)] is flipped 180º in its phase. This phase flip under ideal conditions would cause an inversion of the signal flow; ideally, a mean value of the signal before and after flip would provide the actual zero level of the magnetometer. The idea is the same as when we calibrate a voltmeter zero level by flipping the orientation of a charged battery. This is not so simple for the magnetic sensor, because of the sensors use of high frequency oscillatory currents in the generation of the magnetic field signal measured. As a consequence here we cannot provide a clean MAGCAL evaluation of the instrument zero. But applications of the MAGCAL zero calibration can lead to a reduction of the estimated magnetic field uncertainties. In addition the MAGCAL method provides a check on the health of each magnetic field sensor, oriented along each orthogonal direction in space.

2. Instrument General Characteristics

The geometry of the deployed magnetic field instrument.

The Voyager magnetometer is composed of two sets of sensors at different distances of the spacecraft body (dual magnetometers) (2). They are mounted on the so-called 'Astromast' boom. Each sensor set has three orthogonal oriented flux-gate instruments that measure along each direction the superposition of the 'ambient' magnetic field and the spacecraft generated field. The locations of the sensors in the spacecraft coordinates (3) are given in Table 1:

Table 1

	Inboard sensor	Outboard sensor
X	+ 0.24 m	0.0 m
Y	– 6.52 m	– 11.17 m
Z	– 5.06 m	– 8.98 m

The spacecraft coordinates should not be confused with the magnetic field payload (PL) system defined by the orthogonal direction of each set of three magnetic field sensors in the dual magnetometer relative to the spacecraft.

Time and data set resolution of the magnetic field instrument.

Each one of the sensors in each triad set was oriented originally along the same Cartesian, right handed, orthogonal coordinate axes (payload (PL) coordinate system). After November 30, 2006 the Voyager 2 outboard sensors in the Y and Z PL orientation rotated approximately 58º anti-clockwise around the X PL axis after the sensors were overheated for more than a week as a consequence of a faulty command to a spacecraft subsystem (for a discussion see Section 5). The overheating caused other temporary as well as permanent effects on the Voyager 2 outboard instrument that impact the process of data calibration for the generation of the table of magnetic field zero (zero-offset) values (see Appendix **Method**).

A magnetic field vector sample is measured by the magnetic field instrument every 0.48 sec for each one of the dual vector magnetic field sensors. The high-resolution magnetic field data set, 4 vector averages, has a 1.92 sec sampling rate. This data set and the 0.48 sec raw data are used when performing the electronic calibration of the magnetic sensors (MAGCAL). For the generation of zero-tables 48 sec averages of the magnetic field are used, i.e., the average of 25 1.92 sec B-field vector averages.

The field resolution for each measurement is 12 bits (4096 counts). This same instrument resolution is used for 10 sensitivity levels. At the highest sensitivity level (LFM 0) one step change in the counts means a change in the magnetic field of 0.005 nT. This sensitivity on each sensor determines the limit(s) of the measurements. The field intensities measured in the solar wind beyond Uranus and Neptune often had averaged values close to 0.05 nT, only about 10 times larger than the resolution step of each sensor, and the magnetic field dropped to lower value sporadically. Beyond 83 AU, in the year 2007, the yearly averaged heliospheric magnetic field was 0.04 nT.

The temperature at which the sensor operates

Checking of the sensitivity response to the temperature at which the sensor operates has shown negligible effects for a range of ~300 to 250 K. Currently the magnetic sensors operate at a temperature of ~ 253 K. Early in the mission, near 1 AU, when exposed directly to the Sun light the magnetic sensors reached temperatures of above 300 K. Temperature tests and linearity of the fluxgate magnetometers in the Voyager mission indicate that the calibration stayed at nominal value, since the sensors were calibrated in the laboratory.

On the time evolution of the zero of the magnetometer sensors

Of central interest in the study is the achievement of a zero calibration of each magnetometer sensor with the lowest possible uncertainty. We understand as a 'zero of a sensor' the sensors counts value from

which an observed departure represents an observed calibrated magnitude of the ambient magnetic field. There is a time evolution of the zeroes of the magnetometer sensors. The evolution can be interpreted as a consequence of the sensors systematic errors, and contamination by the variable spacecraft magnetic field.

Noise from the electronics of the instrument can be treated as a statistical error. The statistical error has a decreasing impact through increased larger averages of the measurement of the field.

With a scale from 1 to 4096, 2048 is the nominal 'zero' location for each of the sensors. Nevertheless, the calibration at the laboratory and in flight of the sensors determines the actual location of the zero for each sensitivity level. Table 2 (below) illustrates the value of the Voyager 2 calibrated zeroes at two dates, one in 1981, in the flight toward Jupiter and the other, in 2006, before the solar wind termination shock crossing. Also, the 2006 date is before major disruptions to the outboard Voyager 2 magnetometers caused by a period of extreme overheating, due to a faulty command triggered on November 30, 2006.

Table 2.

Voyager 2	Inboard			Outboard			
Sensor	X	Y	Z	X	Y	Z	date
LFM 0	2074	1695	2083	1915	2046	1935	(9/12/1981)
	2274	1681	2371	1930	2125	1867	(10/30/2006)

The September 1981 values, in Table 2, are from a calibration performed on January 8, 1982 (ref., 4). The recent estimation of Voyager zeroes are the result of roll evaluations in the X, Y payload orientations. A Voyager spacecraft roll is a rotation of the spacecraft around the axis defined by the imaginary line connecting the spacecraft to Earth This line is a direction along the Z-axis (PL) of the spacecraft. Hence, in the Z direction the rolls give zeros of the X and Y components of the magnetic ambient field. The zeros of the Z component of the ambient magnetic field cannot be obtained from the rolls of the spacecraft.

Z zeroes are evaluated using as a first approximation the Parker prediction of average null B-field along the radial component from the Sun. The interval for this Parker assumption is made over two solar rotation (from ~ 25 days before to 25 days after roll). This zero mean value field in the Z-direction is empirical, but it is theoretically supported in the supersonic solar wind region, see e.g. (6). It is a reasonable approximation in the inner heliosheath, but might be less accurate in the distant heliosheath. [Voyager 2 crossed the termination shock into the heliosheath approximately between August 29 and September 1 (DOY 244 to 245), 2007, see e.g. (7), and Voyager 1 has been in the heliosheath since approximately the end of year 2004.

A careful comparison of the signals from the outboard and inboard sensors allows one to identify various spurious perturbations to the location of the zero of the magnetometer. Some of them are the following:
1.- Sudden changes in zero levels locations. They could be related, among other causes, to the sudden change in the spacecraft current triggered by a mode change in the set-up of an engineering mode or a scientific instrument.
2.- Spurious observed changes, possibly due to a bit shift change in the spacecraft telemetry system and to a non steady behavior of specific magnetic sensor(s) electronics. They occur regularly in the Voyager 2 outboard Z and X –axes sensors in the form of spurious waves with variable periods larger than ~40 min to a 10 hours and amplitudes of up to about 20 counts. (These signal variations have amplitudes comparable to the ambient field intensity variations observed beyond 40 AU from the Sun; (Connerney and Kempler, 1989)

3.- The inboard magnetometers on both Voyager spacecraft show also almost the omnipresence of spurious oscillations with a period of ~12.8 min and a variable amplitude with common values of about 2 counts.
4.- In Voyager 1, in addition there is in the inboard Z-axis sensor a nearly permanent spurious noise, which it seems aperiodic (i.e., likely a complex combination of various frequencies) with an almost permanent amplitude of 5 counts.

The above changes would add to the changes produced to the presence of steady currents in the body of the spacecraft, which also influences the location of the inboard and outboard zero level.

The Z-zeroes in the heliosheath, after the crossing of the termination shock (TS).
In the region beyond the heliosphere the Voyager 1 and 2 the assumption of a zero mean in the radial magnetic field over 2 solar rotations is unsupported at present. Nevertheless, as a first approximation, the Parker zero-mean magnetic field assumption is further used. However, it is corrected to be consistent with the observed time structures in the three field components, which are naively interpreted to be compressional features, i.e., when $\Delta B_x/B_x = \Delta B_y/B_{y,}$ it is assumed that the relationship also holds for the 3rd component, i.e.,

$$\Delta B_x/B_x = \Delta B_y/B_y = \Delta B_z/B_z$$

Field values evaluated in this way are further subject to a constraint based on using electronic magnetic calibration (MAGCAL) data, performed approximately every 29 days In the next section we investigate the limits that these MAGCAL tests set on average uncertainties of the B-field zero evaluations.

3. The electronic calibration test and its uses in the determination of the signal uncertainty

An electronic sweep of all sensitivity levels (LFM0 to LFM7, and HFM LO, HFM HI) is performed approximately every 29 days, about 13 times a year (not shown in Figure 1). After the end of the sweep the instrument is stepped through the changes (a 'MAGCAL') shown in Figure 1.

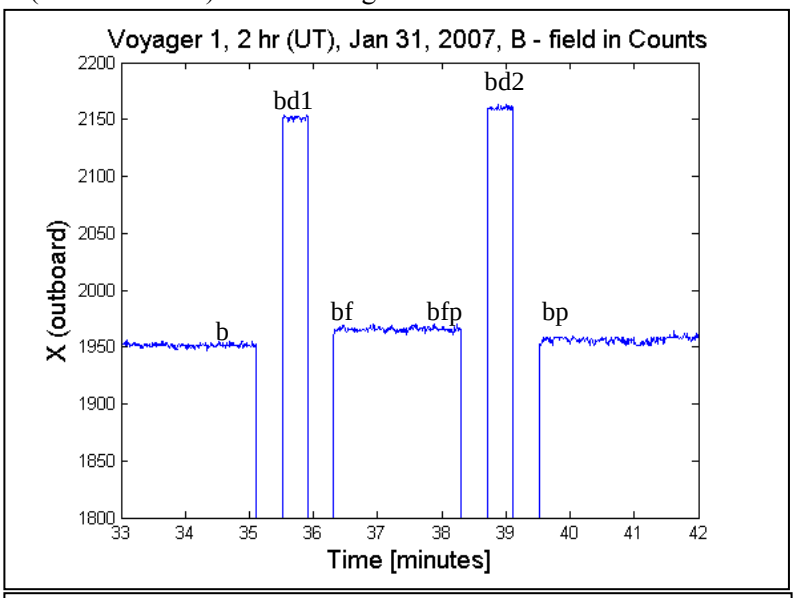

Figure 1. The X (*outboard* signal in counts) dependence on time, is plotted for four different status of the sensors electronic, see text.

First the phase of the core's coil is shifted by π. (the signal jumps from 'b' to 'bd1'). Second the external coil phase is shifted by π (the signal jumps from 'bd1' to 'bf'). Third the cores coil phase is back to its regular value (the signal jumps from 'bfp' to 'bd2'), and fourth the external coil phase is shifted back to its original value (the signal jumps from 'bd2' to 'bp'), restoring normal operation of the sensor. The time scale shows that the MAGCAL operation takes 5 minutes (from 35 to 40 minutes after 2 UT, in January 31, 2007). For this interval Figure 1 shows the high resolution raw data (i.e. sampled at a rate of one vector every 0.48 sec).

The ≅ 2 minute interval between'bf' and 'bfp' shows the signal sampled at the reversed phase relative to a regular sample ('b').
If we can assume that the instrument is free of any magnetic coupling and that the ambient signal and the spacecraft field has not changed from minute 35 to minute 40, then *the zero* of the instrument would be located at

$$0_{Bx} = ½ (b + bf) \qquad [1]$$

(for the X PL oriented sensor), or at a weighted combination such as

$$0_{Bx} = ½ \{½ (b + bp) + ½ (bf+bfp)\}$$

The assumptions for these simple relationships appear to be supported by the display of 'b'(crosses connected, with solid blue line) and 'bf'(crosses connected with solid green line) in Figure 2.
Notice the mirror symmetry among the 'b' and 'bf' values.(this is the inboard sensor Yin oriented in the Y PL direction. as a function of time in the instrument in Voyager 1.)

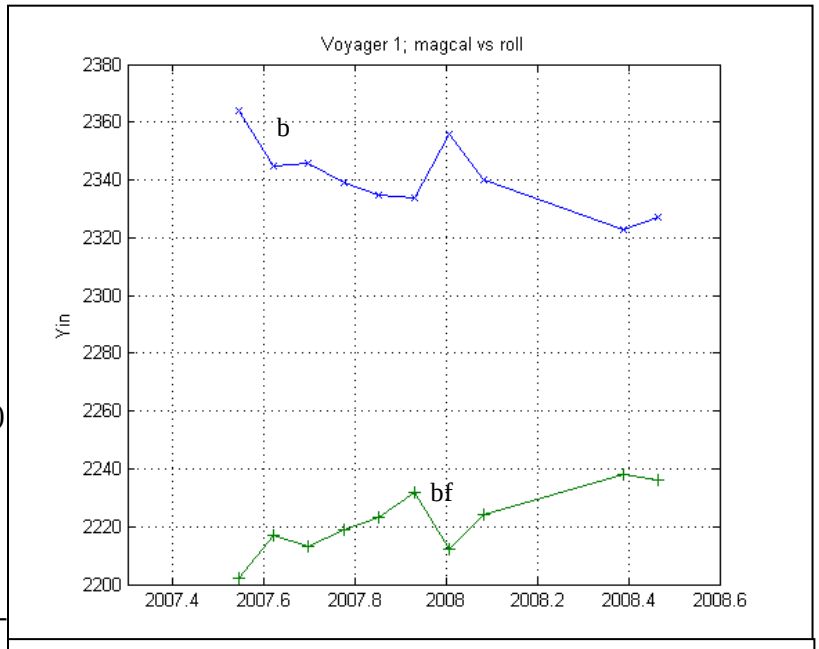

Figure 2. The Y *inboard* signal (Counts) for two sensor conditions (normal b: blue, reversed phase bf: green) as a function of time (Year).

For the zeroes derived from the same time interval we compare these observations with the accurately estimated zeroes (0_{Yin}) obtained by rolling of the spacecraft around an axis pointed in the Z PL direction (the imaginary line connec-

ting Voyager with the Earth).

Figure 3, below, illustrates a situation different from the one predicted by Equation (1). With the zero of the Yin-sensor (0_{Yin}) displaced toward the 'b' curve. The figure also shows zero values computed from 'b' and 'bf' using three different weighted averages.

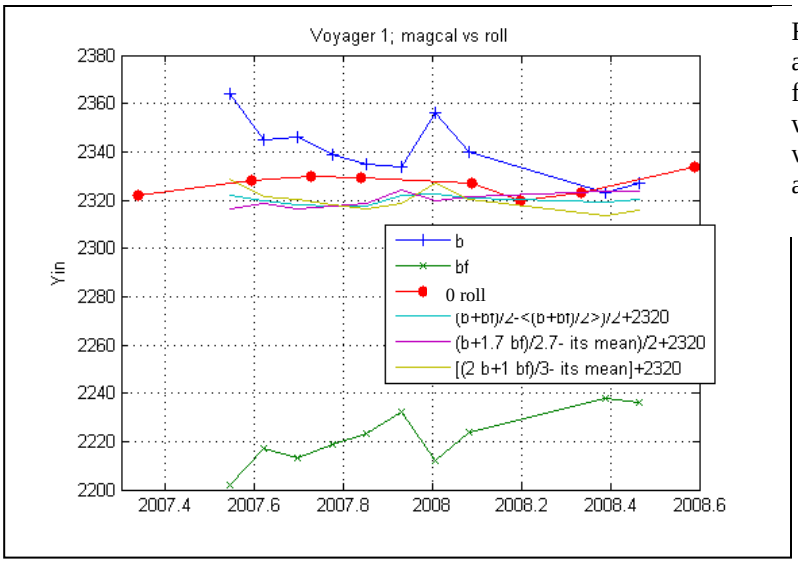

Figure 3.Same as Figure 2 but including the ambient zero field calculated using data from the roll, the red solid circle connected with red line. Three different 'normalized' weighted averages of the 'b' and 'bf' signals are also shown.

When a *change in state of the sensor* takes place the preceding assumption, do not apply. Naturally such a change affects the zero of the sensor as illustrated in Figure 4 for the Voyager 1 outboard sensor oriented in the X PL direction.

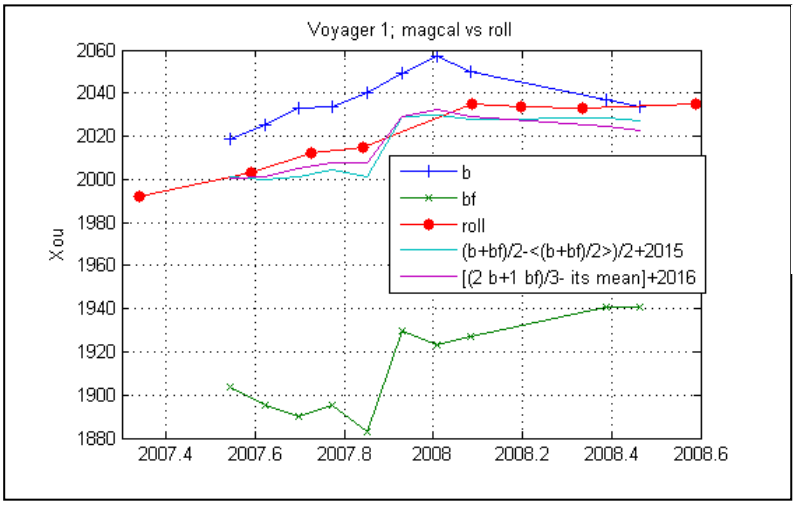

Figure 4. Like Figure (3), but for the X *outboard* sensor.

The Xou from the roll and the MAGCAL shows a jump in the zero levels different weightings of the Xou 'b' and 'bf' reproduce quantitatively the size of the jump in the location of the zeros provided by the rolls. Notice that the higher frequency in the MAGCALs compared to the rolls narrows the location in time of the *change in the* Xou *sensor state* (jump). As the arrow in Figure App **Method** 1 indicates, a comparison of the inboard and outboard magnetometers allow one to narrow the temporal interval of the location of a 'sudden' change in the location of the 0_{Xou} or the zero of any other sensor.

It was found for Voyager 1 X PL and Y PL directions that

$$0_{Baxis} = 1/3\,(2\,b + bf) - \langle 1/3\,(2\,b + bf)\rangle + \text{Norm Constant} \qquad (2)$$

appears to give the most accurate description of the location of the zero level determinations by rolls for the approximately year long interval analyzed here. The average displacement of Equation (2) respect to roll values is about 9 Cts. Departures for extended intervals (greater than two weeks or more) are well below 20 Cts (~ 0.1 nT).

We extend these procedures to the Z direction, where no roll for zero calibration is possible.
Iin the case of the Z direction, we compare the corresponding MAGCALs relations (1) and (2) to our best empirically $0_{Zin/out}$ estimates, in Figure 5.

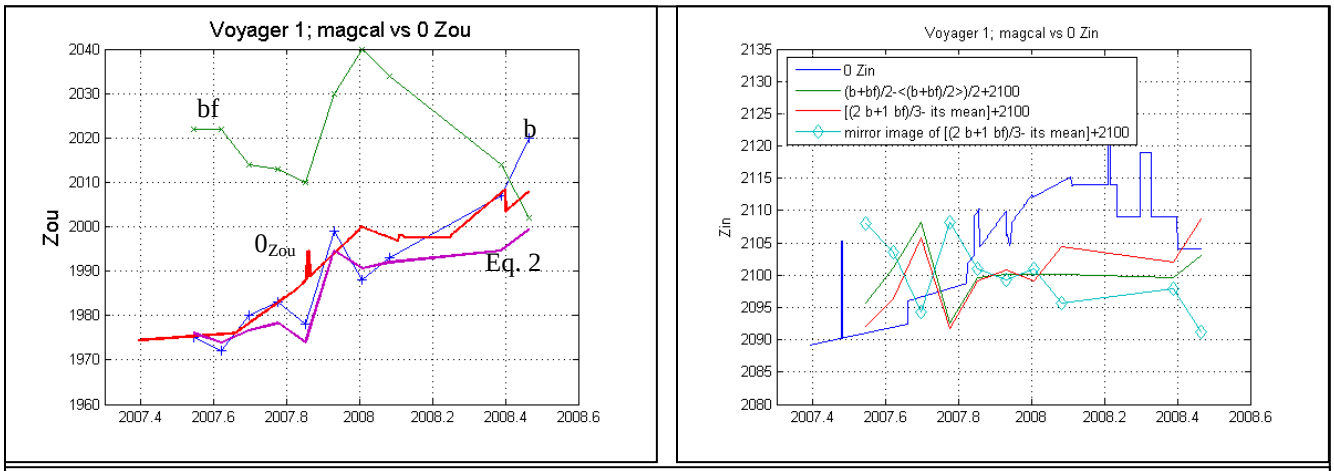

Figure 5. On the left panel we plot 1) the Z *outboard* regular signal 'b' (Counts) as a function of time (blue): 2) the phase reversed signal 'bf' (green), the estimated ambient field zero Z component (orange). The weighted average of 'b' and 'bf'(violet). The right is same as the left panel but for Z *inboard,* with blue for the estimated ambient field zero Z, green, orange and turquoise for different weighted averages of 'b' and 'bf'.

Figure 5 (left) for the outboard Zou direction, shows that the weighting in Equation (2) between 'b' and 'bf' give a reasonable quantitative approximation to the estimated 0_{Zou} with Norm Constant = + 1985 Cts.

For the inboard sensor Zin, the Figure 5 (right) shows a less clear behavior. Nevertheless points calculated (connected with orange line) give values close to within approximately 12 counts of the estimated best 0_{Zin}. Notice that in this case the behavior of 0_{Zin} is strongly distorted in a range of ~ 15 Cts, and in an apparently skewed way by the presence of a nearly permanent, complex electronic, aperiodic spurious variation in the analyzed one year interval (e.g., the noisy *inboard* signal in Figure 14).

Figure 6 shows *the Electronic calibration* (MAGCAL) *of the Voyager 2* for the same time interval. Points computed as using Equation 2 are shown in comparison to 'b' and 'bf', and the roll values for Xou and Xin.

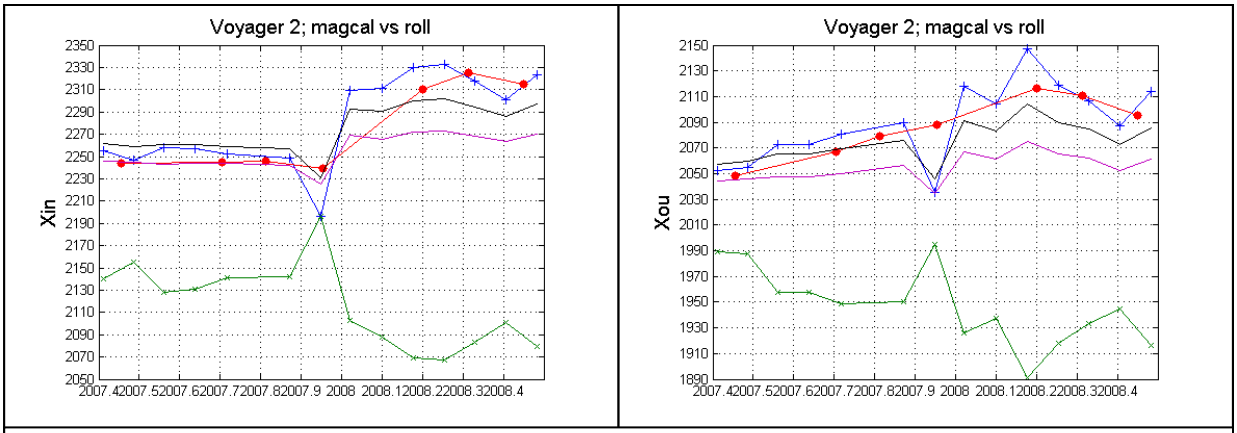

Figure 6. On the left X *inboard* (Counts) as a function of time (Year) in blue for 'b'; green for 'bf'; red for the zero roll values, violet for Equation 2 weighting of 'b' and 'bf', and black for Equation 3 weighting of 'b' and 'bf'. On the right same for X *outboard.*

As in the case of Voyager 1, the differentiated weighting of 'b' and 'bf" provide a reasonable representation of the location of the 0_{Xaxis} both for the outboard and inboard sensors. Now, the weighting

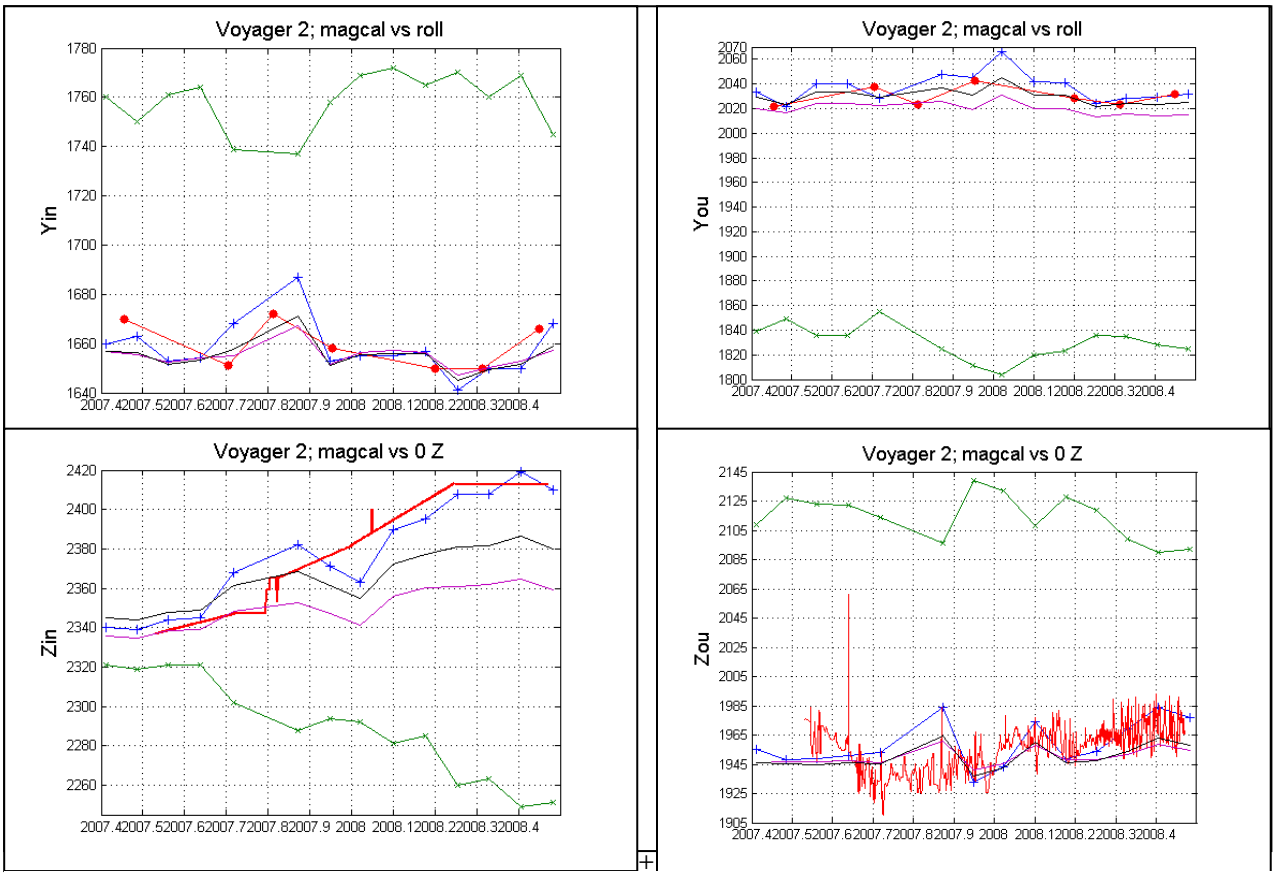

Figure 7. Same as Figure 6, but in the bottom panels the red line is the estimated zero of the ambient field.

The points connected with a black line in Figure 6 appear to be favored, from a quantitative point of view.

This is the case for the 0_Y and 0_Z axes for both inboard and outboard sensors, i.e., Equation (3) appears to be a more accurate representation of the magnetic field zero of the respective sensor. Nevertheless, the quantitative agreement is now within 12 Cts. This is slightly less that in the MAGCAL relationships for 'b' and 'bf' found for Voyager 1. Hence we also explored other combinations, finding that

$$0_{Baxis} = \tfrac{1}{2}\,[\tfrac{1}{2}\,(b + bp) - bd2] \quad + \quad \text{Norm Constant} \qquad (4)$$

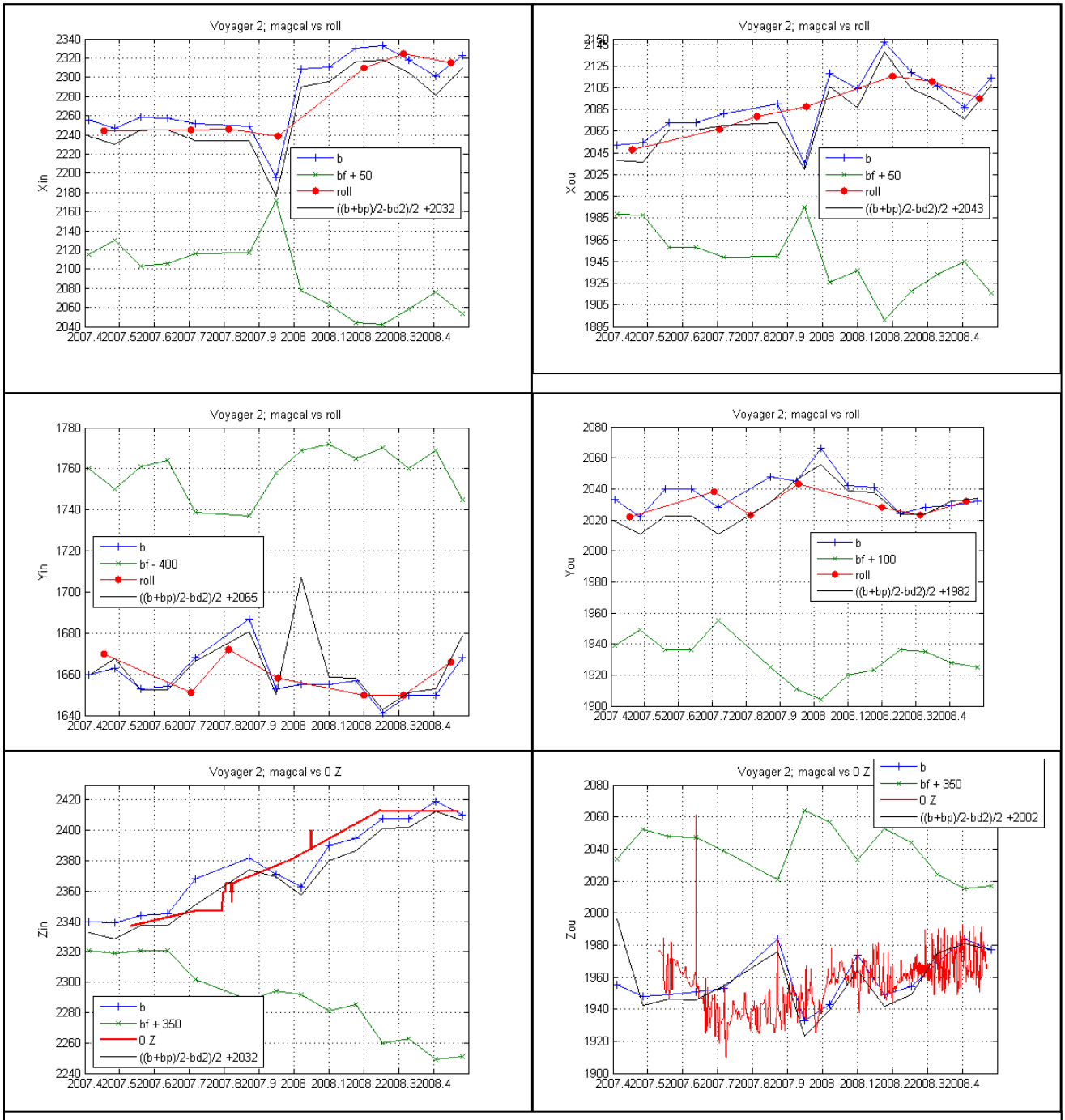

Figure 8. Top panels same as Figure 6. Middle and bottom panels same as in Figure 7.

i.e. ~ 0.1 nT of the best estimate. This is comparable to the result obtained using Equation (3). This useful result is illustrated for each axis sensor in Figure 8.

4. The standard roll calibration

When the spacecraft rotates slowly around the Z PL direction, i.e., the axis connecting the spacecraft with Earth, the tip of a constant ambient magnetic field vector, projected in the X-Y PL plane, draws a perfect circle. This condition is partially satisfied most of the time. By the same reasoning X and Y PL components of the measured ambient magnetic field sense sinusoidal signals (see Figure 9, below) as a function of time. Thus a roll allows a precise measurement of two components of the 'ambient' field from the signal observed with the magnetic field instrument, during the roll, when the ambient field is ~ constant.

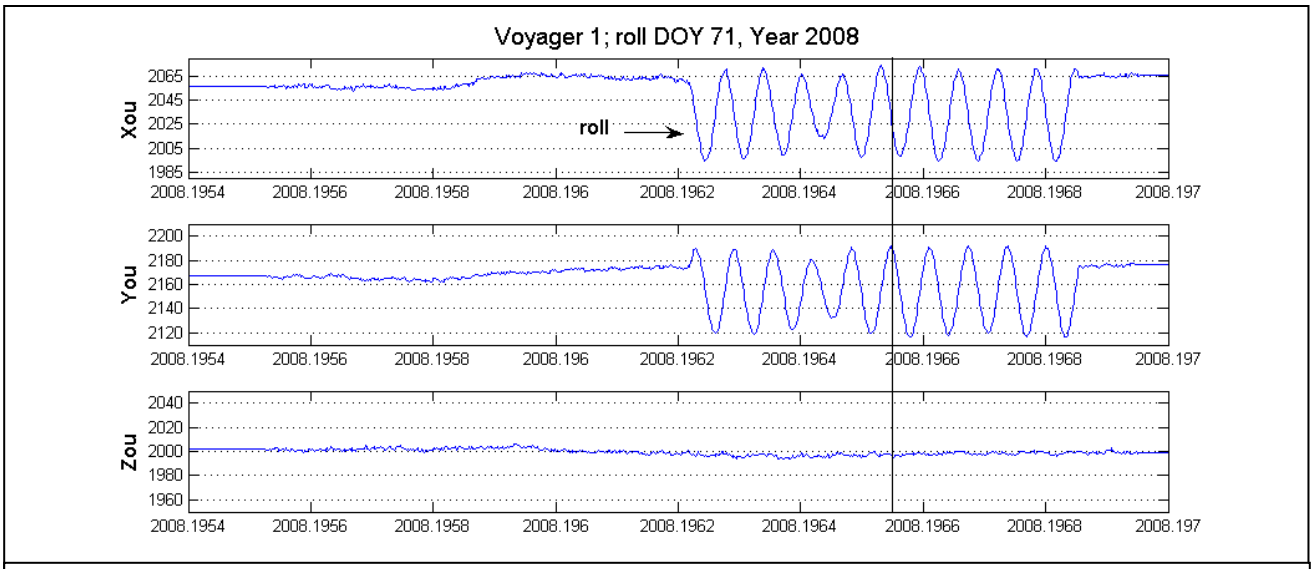

Figure 9. top panel shows the X *outboard* field signal as a function of time (Year) during interval of time containing 10 consecutive 'rolls' of the spacecraft. Middle and bottom panels show Y and Z *outboard* field signals during the same time interval.

The determination of zeros using a roll is illustrated in Figure 9. The vertical line marks the approximate value (2026 counts) for the zero in the direction of the X PL sensor. The identified zero in the signal measured in the X PL sensor corresponds to the apex value for the Y PL sensor. During the 30 min 14.4 sec of the slow period of rotation we have a sinusoidal signal! The 10 rolls (counted from the peaks in the Xou or You curves) give a very accurate estimate of the zeroes using this technique for both outboard and inboard sensors. As discussed above there is no effect of the roll on the Z direction. Notice that the sensors show a stronger signal (temporal magnetic field variations) both in the X and Y PL directions than in the Z PL direction (Notice that considering the vector nature of the field, a lesser signal variation in a direction would indicate a field with its smallest component in that direction.)

Figure 9 shows an interval of 'strong' fields (~ 0.18 nT as corresponding to 36 Cts 0.005 nT/Cts) in the heliosheath. During the time of the roll, the field strength and/or direction changes. Nevertheless, the method gives us a large number of vectors (~400 samples) with enough statistic to accurately estimate the location of the zeroes to less than one count uncertainty (~0.005 nT) for the sensors along the X and Y PL directions.

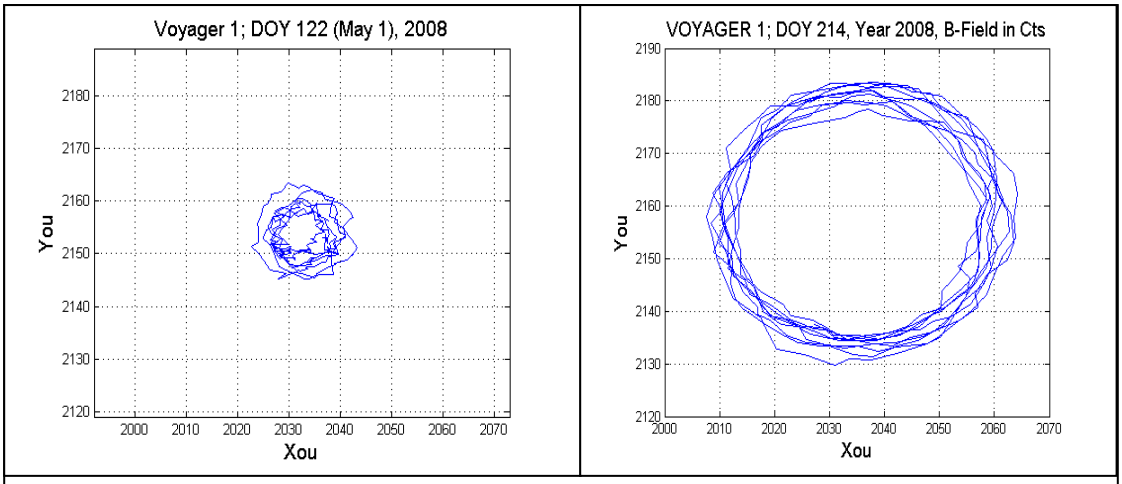

Figure 10. Representation of the *outboard* magnetometer Y field signal as a function of the X signal during a roll interval (in Count units).

The statistical method of evaluating the mean of ~200 instantaneous gyration radii determined during 10 spacecraft roll rotations has a resolution of a fraction of decimal that we round to the nearest natural number. In the case of the three rolls discussed here, the zero X and Y PL values for the outboard sensors are the following:

Table 3

Outboard Sensor	DOY 071	DOY 122	DOY 214
X zero	2034	2033	2035
Y zero	2154	2154	2158

We emphasize that the zero evaluation from the roll cannot give the zero for the component along the Z PL axis of the spacecraft.

5. Calibration of the Instrument using a 0.5 Amp driven, onboard, large radius coil.

An in flight calibration of the instrument scale is provided by the observation of the field generated by a large coil build in each Voyager spacecraft. This field also allows determine the exact orientations of the inboard and outboard magnetometer (5). A test of the outboard sensors was made to identify a rotational displacement of the outboard Y and Z PL oriented magnetometers in Voyager 2 after the heater incident. This test allowed the determination of their orientation and field sensitivity in year 2007.

In the spacecraft coordinate system the coil current produces a known dipole field at the location of the magnetic field sensors. The coil is mounted on the external circle of the main parabolic spacecraft antenna with its center at the position in Table 4.

Table 4.

Antenna	Location [m]
X	0
Y	0
Z	-1.58

The diameter of the antenna is 364.9 cm. The coil consists of 20 turns of #26 wire carrying a continuous current *I* (1/2 Amp being the originally tabulated value) when active. Table 1 gives the location of the inboard and outboard sensors in the spacecraft system. The coil plane is perpendicular to the spacecraft Z-axis to within ±0.25°. From Tables 1 and 4 we obtain the coordinates of the inboard magnetometer relative to the center of the coil:

$$\Delta r_{inX} = 24\text{cm}, \quad \Delta r_{inY} = -652\text{ cm}, \quad \Delta r_{inZ} = -506\text{ cm}, \qquad (5)$$

and of the outboard magnetometer relative to the center of the coil

$$\Delta r_{ouX} = 0, \quad \Delta r_{ouY} = -1117\text{ cm}, \quad \Delta r_{ouZ} = -740\text{ cm}, \qquad (6)$$

In this way it is possible to give precisely the magnetic field at the location of each one of the magnetometers. For the determination of the model magnetic field values see Appendix '**Mag Dipole**'**.** Figure 11 shows the effect of the current activation on the observed fields.

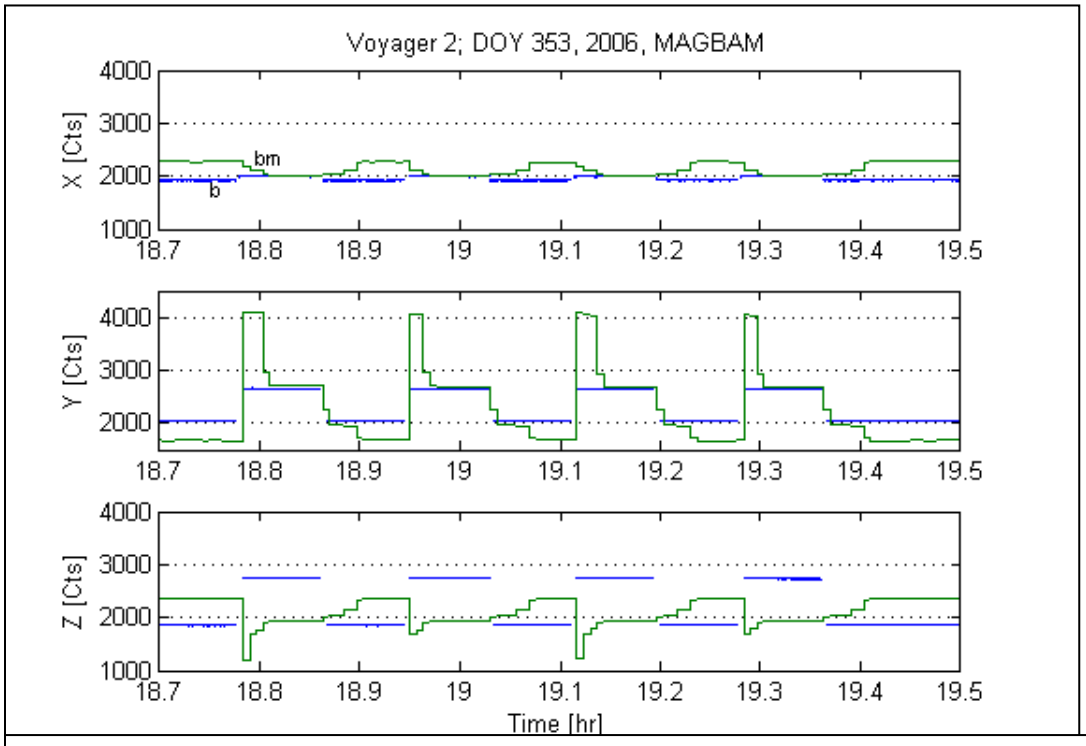

Figure 11. The *inboard* and *outboard* field signals as a function of time (hours) during a set of four MAGBAM

The blue line, a step function (observed more easily in the bottom panel) indicates four activations of the spacecraft coils magnetic field. There is in average 24.8 sec between the 8 up and down steps (blue line). This results indicates that the detector responds within at least ~25 sec to a large (few nT) sudden field change, and even faster (~1.92 sec) to a more gradual field variation. The field interval when the coil field is not active is labeled 'b' in the top panel; and when it is active it is labeled 'bm' (for the MAGBAM field of the coil present).

When we first activate the coil, the green curve in Figure 11 shows a more complicated evolution of the inboard magnetic field. This occurs because of a coil generated, magnetic field at the *inboard* magnetometer approximately a factor 5 stronger than that at the outboard sensors. Therefore, at the *inboard* magnetometers there is a stepping of each sensor from the more sensitive level (LFM 0) to the second level (LFM 2). Also the inboard sensor has a time resolution of one sample every ~12 sec (see the overall step signal shown by the green curve). The consequence is that, at the end of each 5 min MAGBAM active coil interval, each inboard sensor gives the most accurate signal for the zero of the LFM 2 sensitivity level, before stepping back to the zero sensitivity level LFM 0. The LFM 0 level is active for the ambient field far from the Sun. (This is true even at 5 AU or even less, depending on solar wind conditions.)

Figure 11 further shows that the coil appears to generate the smaller changes in the X direction, for which a nominal zero change was expected, because of the designed orientation of the magnetometers (Payload coordinates) relative to the coil. The other coordinates show comparable values for the outboard components You and Zou while the inboard fields appear to be more dominant in the Yin than in the Zin direction.

As expected, the difference in strength among the field components of the inboard sensors appears to be consistent with the known orientation of the detectors since the start of the mission. A detailed view of this observation in Figure 11 is presented below, with a closer look to the Y and Z fields at the end of a coil activation cycle, see Figure 12.

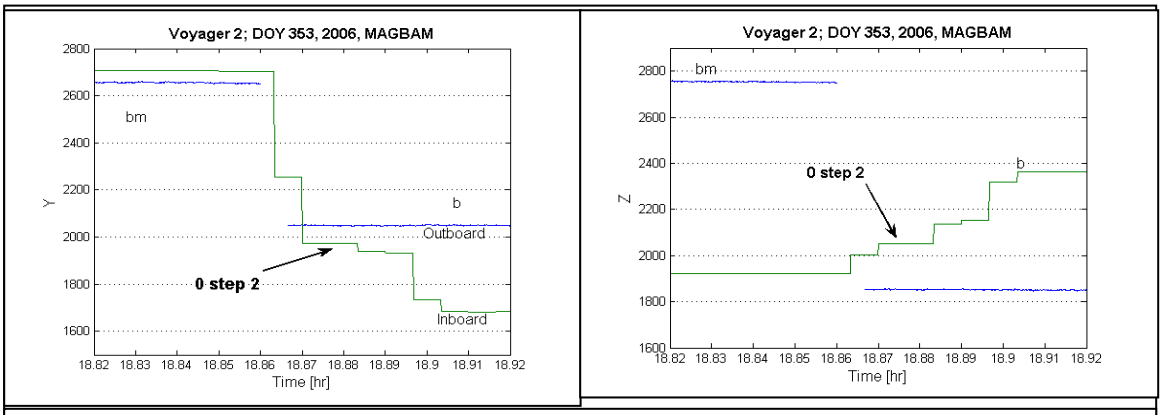

Figure 12. Detail of the *inboard* and *outboard* MAGBAM transition from active coil field to non-active coil field as a function of time for the Y and Z field sensor signals (in Counts) as a function of time [hour].

Figure 12 shows the Y-Z PL magnetic field signal versus time. On the left of each panel it is the component signal 'bm', recorded when the current '*I*' in the coil generates a well known magnetic dipolar field at the locations of the inboard and outboard magnetometers (see Appendix '**Mag Dipole**'), which is turned off between times 18.87 and 18.88 (hr). Hence, the blue line on the right (time >18.86 hr) gives the ambient magnetic field component ('b'). Hence, the difference

bm – b

represents in Counts the measure of the magnetic field for the *outboard* magnetometer (blue line). Because the *inboard* magnetometer coil field is closer to the coil, its magnetic field is measured at the sensors 2nd sensitivity level (LFM 2). Thus,

bm – b(18.865 hr), with ‘b’ = the step-like value labeled ‘**0 step 2**’ in Figure 12,

represents in Counts the measure of the magnetic field for the *inboard* magnetometer (green line). The values, counts obtained in these way, are easily converted to ‘nT’ using the sensitivity factors listed at the bottom of the Table 5. This Table shows the results obtained from the analysis of the data illustrated in Figure 11.

Table 5. Mean inboard magnetic field, after overheating of the *outboard magnetometer*.

Year DOY	Inboard	magnetic	field in	Cts	magnetic	field in	nT
Time		X_{in}	Y_{in}	Z_{in}	B_{Xin}	B_{Yin}	B_{Zin}
2006 353	zero level	2030	1972	2053			
19 UT	coil field	2022	2694	1924	-0.361	30.57	– 5.50
2007 129	zero level	2027	1971	2049			
05 UT	coil field	2019	2693	1920	-0.361	30.57	– 5.50
					nT/Cts	*nT/Cts*	*nT/Cts*
Magnetic	Field	sensitivity	level	LFM 2	0.0452	0.0423	0.0426

A comparison of the values of the inboard magnetic field after DOY 335, 2006, with the values obtained in the earlier stages of the mission is given in Table 6.

Table 6. Mean *inboard* magnetic field before and after on DOY 335, Year 2006.

Inboard	magnetic	field in	nT	
	B_{Xin}	B_{Yin}	B_{Zin}	$\|\mathbf{B}\|$
Early mission (EM)	– 0.173	23.85	– 4.37	24.25
This evaluation (TE)	– 0.361	30.57	– 5.50	31.06
Ratio B_{EM}/B_{TE}	0.48	0.78	0.79	0.78

The approximately *same* B_{EM}/B_{TE} ratio for the Y-Z PL coordinates suggests that the orientation, of the *inboard* magnetometer was the same before and after the overheating of the *outboard* magnetometer. The uncertainty in the evaluation of the weak X PL signal may be the explanation for its approximately 50% smaller B_{EM}/B_{TE} ratio. (It is possible that earlier in the mission it was more difficult to separate the weak (fraction of nT) zero in the X direction from changes in an ambient mean field of a few nT near the Earth.)

At the *outboard* detector location the magnetic field is always in the measurement range of the highest sensitivity level (LFM 0) (see Figure 11). This condition allows us to estimate the *outboard* magnetic field at the turn on and off of the current in the coil, strongly increasing the statistical accuracy of the field determination.

Table 7. Mean *outboard* magnetic field before and after on DOY 335, Year 2006.

outboard	magnetic	field in	nT	
	B_{Xou}	B_{You}	B_{Zou}	$\|\mathbf{B}\|$
Early mission (EM)	– 0.003	4.136	– 0.223	4.142
This evaluation (TE)	0.363	3.012	4.271	5.239
Ratio B_{EM}/B_{TE}	– 0.008	1.37	– 0.05	0.79

Table 7 shows the departure of the ratio B_{You}/B_{Zou} = 0.705 at 'this evaluation' (TE) from the ratio B_{You}/B_{Zou} = -18.547 in the 'early mission' (EM). This change confirms that the *outboard* Voyager 2 detectors rotated as a consequence of their overheating during a several days interval near DOY 335, 2006. These results are confirmed by the BAGMAN test on DOY 129, 2007, within the sensitivity of the magnetometer, i.e., ~0.005 nT. Tables 6 and 7 show that the magnitude of the coil magnetic fields have the same ratio in strength between the determination in the 'early mission' (EM) and 'this evaluation' (TE), supporting the assumption of a higher conductivity at the time of 'TE' because of a reduced coil resistivity owing to a much lower temperature in the Sun illuminated antenna at approximately 80 AU from the Sun than within a few AU during the EM. The indicated shift in orientation relative to the original deployment is

$$\arctan(B_{Zou}/B_{You})TE - \arctan(B_{Zou}/B_{You})EM = 54.82° + 3.08° \cong 58° \quad (7)$$

We use this angle to correct the *outboard* signal after DOY 345, year 2006. As an example, Figure 13 shows that the correction gives agreement of the signals observed in the *inboard* and *outboard* magnetometers during rolls (see Figure 13).

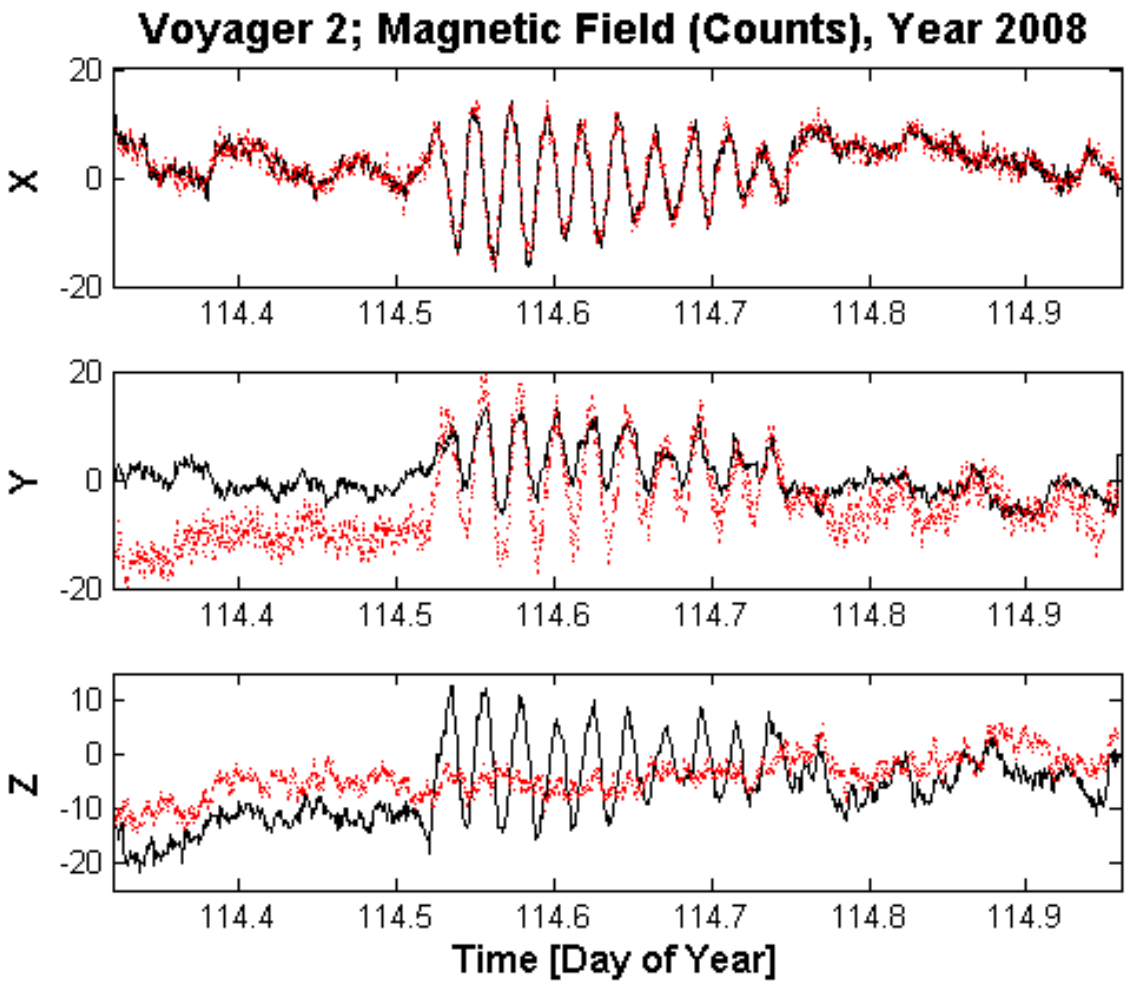

Figure 13a. top panel shows the X *outboard* (black) and *inboard* (red) field signals (Counts) as a function of time during interval of time containing 10 consecutive 'rolls' of the spacecraft during a roll. Middle and bottom panels show Y and Z *outboard* field signals during the same time interval rotation.

The rotation of the processed signals along You and Zou (black curves in central and bottom panels in Figure 13a) uses the following relationships.

$$B_{Zou}\,(PL) = B_{Zou}\,cos(\theta) - B_{You}\,sin(\theta) \quad (8a)$$
$$B_{You}\,(PL) = B_{Zou}\,sin(\theta) + B_{You}\,cos(\theta) \quad (8a)$$

with $\theta = 58°$. In this way now the obtained B_{Zou} (PL) and B_{You} (PL) that agree with the corresponding value for the X and Y PL components fo the inboard magnetometer, illustrated below (Figure 13b).

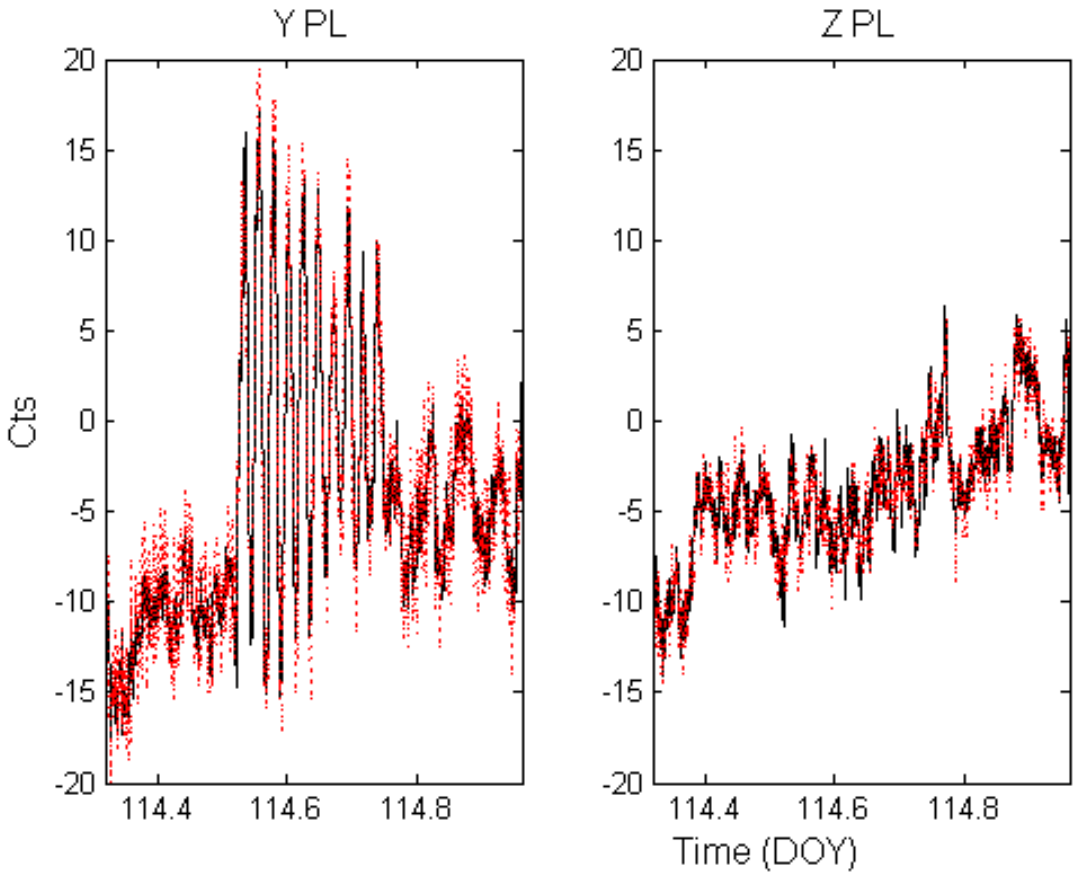

Figure 13b.Left panel shows the Y payload *outboard* (black line) and *inboard* (red dotted line) as a function of time for same time interval as Figure 13a. Right panel is same as left but for Z payload *outboard* and *inboard* magnetic field signals.

In addition Figures 13a and 13b show the close agreement in the sensitivity (LFM 0) for each of the sensors (inboard and outboard) of Voyager 2. The data shown in Figures 13a and 13b have been cleaned from the presence of spurious wave activity. This spurious wave with a period of approximately 12.8 min is characteristic of all Voyager inboard detectors.

Often, in the outboard X and Z sensors, there is another type of spurious signal. This signal can be as large as ~20 Cts in amplitude. It has a slow but variable period (> 30 min), which often appears to be triggered during rolls (see Appendix **Method**). Figure 13b (left panel) also shows the presence of a larger residual 'noise' in the *inboard* signal, along the Y PL axis.

6. The estimation of the B_Z using a 'compressive plasma' arguments.

Once the calibration is complete we investigate the possibility of detecting and correcting shifts in the Z PL direction, where no roll or absolute estimate of the field is possible. This direction is radial from the Sun, and in the interplanetary solar wind, is on average zero (7). In the heliosheath region this assumption needs to be tested.

As an alternative to using the MAGCALs to constrain the radial magnetic field component relative to the Sun, B_z, we perform routine checks of the PL coordinate system in both spacecraft trying to identify intervals which are reasonably best candidates to be compatible with magnetic field showing good 'compressive plasma' structures in the X and Y PL directions. This means to assume that the field satisfies the condition $\Delta\mathbf{B} \sim \mathbf{B}$. The Figure 14 illustrates one of those many cases.

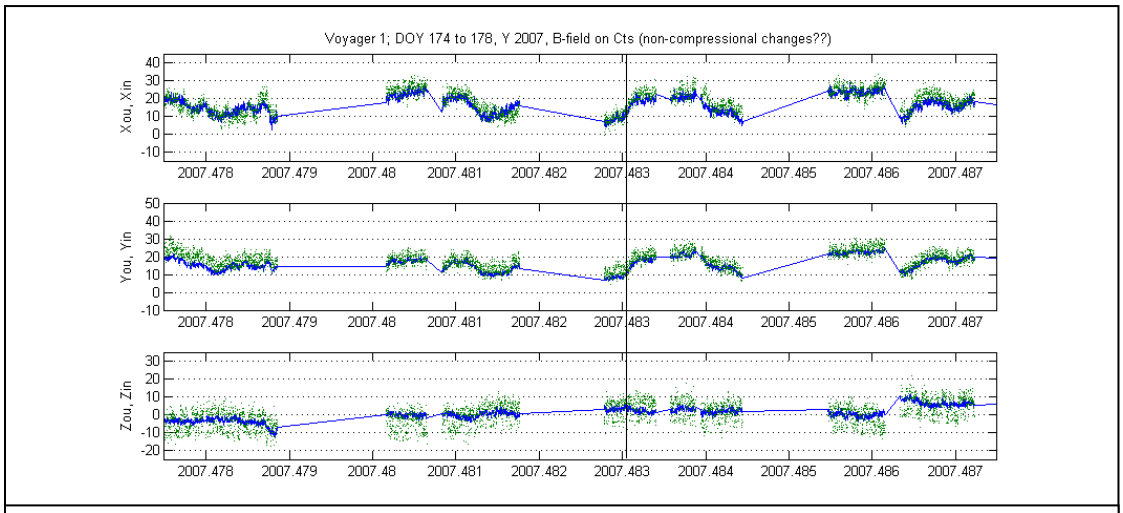

Figure 14. Top panel shows the signal for X *outboard* (blue line) and *inboard* (green dots) as a function of time (Year). Middle and Bottom panels show same for Y and Z sensor signals.

The vertical line shows the location where it is possible that the field may be compatible with a *compressive plasma* structure. In that case the positive changes in the X and Y PL directions would be accompanied by an intensity increase in the Z PL direction proportional to the intensity of the magnetic field. (i.e., at larger field intensity in a direction with larger variation) The smaller signal changes for the time following the vertical line are consistent with the lower intensity in the Z direction. Also the direction change implies a weak, *negative*, B_z component. Therefore, the assumption of the *compressive plasma* structure is consistent within two or three counts (~ 0.012 nT) with the location of the zero line for the Z-axis.

An example of this *compressive plasma* structure correction to the Z zeroes to the Parker evaluated zero offset follows. For the interval illustrated below (DOY 170 to 177, 200) taken from a survey of a longer time interval, there are two regions marked with vertical lines. The time series near the vertical line in both cases are consistent with the *compressive plasma* assumption is not satisfied in the Z direction. Figure 15 is an example of this correction.

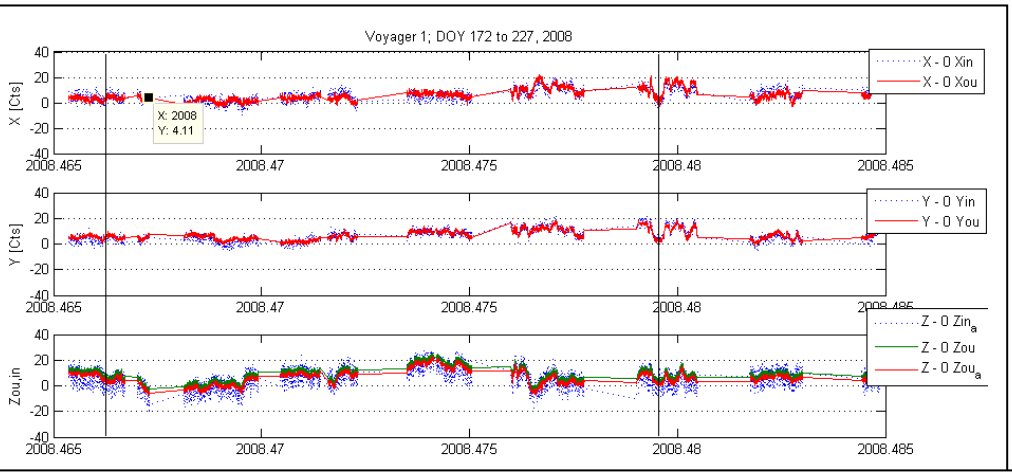

Figure 15. Top panel shows the signal for X *outboard* (red line) and *inboard* (blue dots) as a function of time (Year). Middle panel shows same for Y sensor signals. For the Z sensor signals the *inboard* signal is again the blue dotted points. The Z *outboard* green line is the Parker zero adjusted signal ($<B_{Z\,PL}> = 0$ for 2 solar rotations), and the green line gives the zero Parker modified, as discussed in the text.

However, the starting Parker estimate for the zero line in the Z-axis direction appears too large to be compatible with the *compressive plasma* conjecture. In this case the red line in the bottom panel of Figure 15 shows that now the field is consistent for the time series, within two to three counts uncertainty with the *compressive plasma* conjecture.

These adjustments of the Z-axis field component are made when $\Delta\mathbf{B} \sim \mathbf{B}$, features appear to be valid. Thus, we do overall corrections to the Z-zeroes estimated using Parker assumption when the '*compressive structure'* condition appears well satisfied for short time intervals like the ones shown in the examples. These intervals are used for correcting the Z zeros evaluated using Parker.

7. Conclusions

The analysis presented in Section 3 shows that we can use the analysis of the intervals of phase inversion in the sensors of the dual (*inboard and outboard*) magnetometers to set conservative 'MAGCAL' limits to the deviation from actual ambient magnetic field values.

Our finding, illustrated with Figures 3 to 8 is that accurate roll zero values for the ambient magnetic field in the X and Y payload (PL) directions are within less than 40 Counts (1 count → 0.005 nT unit) from the unmodified 'b' signal in the 2007-2008 year time interval. This, combined with the finding that the relationships found with the signal recorded when sensors operational phase is reversed 'bf', is less than

12 counts from the values obtained from rolls for extended periods of time. This analysis with MAGCALs is extended to the sensors of the dual magnetometer oriented along the Z-axis, (the axis of roll rotation, and in this way set an error limit of ~ 0.06 nT = 12 Cts × 0.005 nT/Cts.

Assuming the validity of the *compressive plasma* conjecture this limit to the possible shift of the zero ambient field component of the instrument for the Z direction can further be reduced to a few counts, in most cases ~ 0.015 nT as it is shown in the section before, Section 6.

An important test of the experiment is the regular checks on the accuracy of the sensitivity of the instrument by repeated test of the signal through the integral analysis and comparison of the recorded data with the *inboard* and *outboard* detectors. This is performed not only at rolls (Section 4) but for each whole interval between rolls. Due to the so called HYBIC accident –the overheating of the outboard magnetometer in the Voyager 2 mission beginning at DOY 335, 2006– we performed a renewed test of direct calibration of all magnetometer sensors and their orientation. The results confirm the quality of the operational sensitivity of the instruments. These results, discussed in Section 5, further allowed to accurately determine the new orientation of the *outboard* Y and Z labeled detectors which now are rotated 58º relative to the Y and Z PL directions of the instrument.

Section 6 presents examples of a jump, spike like, spurious signal that cannot be addressed simply. The presence of these spurious data is less common in the Voyager 1 than in Voyager 2. Its presence must be identified and to remove by carefully comparing the time series of both magnetometers. Its presence shown here for 48 sec averages could in some cases affect the data for hour averages. The Appendix **Method** presents a more thorough discussion of spurious elements in the signal and their corrections

Finally we note that both spacecraft see a signal that shows more change range in their hour-daily to monthly variation in the directions transverse to the direction defined by a line connecting the Sun to the spacecraft. This is also the case after the crossings of the termination shock by Voyager 1 and 2. This weaker magnetic field activity along the Z PL direction is further evidence that the component of **B** in the radial direction is less than in the transversal components. (We assumed $\Delta\mathbf{B}_z \sim \mathbf{B}_z$, see Section 6.)

Appendix '**Mag Dipole**'

The symmetry of the coil source gives only a radial and axial dependence of the spherical coordinates distance *(r)* and colatitude *(θ)* of the **B**-field. The exact expression

$$B_r = (2\pi Ia^2)/(cr^3) \sum_n (a/r)^{2n} (-1)^n (2n+1)!!/(2^n n!) P_{2n+1}(\cos\theta)$$

$$B_\theta = (\pi Ia^2)/(cr^3) \sum_n (a/r)^{2n} (-1)^n (2n+1)!!/(2^n [n+1]!) P^1_{2n+1}(\cos\theta)$$

with $B_\phi = 0$ *and* $0 \leq n < \infty$, shows an expansion which scales with $(a/r)^2$ where a = 364.9/2 cm (the radius a of the coil) and r = 739.45 (1340) cm for the inboard (outboard) locations (Gaussian system of measurement (8). Here, the positive sign in B_θ *is correct*), θ = 61.93° (56.48°) is the inboard (outboard) axial angle defined in the Y-Z PL plane, exactly for the outboard and within 1% for the inboard magnetometers. It is easy to show that the 3rd term in the expansion will contribute an O 0.5 10^{-3} (10^{-6}) for the inboard (outboard) magnetometer. Hence, the above general expressions reduce to

$$B_r = (2\pi Ia^2)/(cr^3) \{ \cos(\theta) - \tfrac{3}{4} (a/r)^2 (5\cos^3(\theta) - 3\cos(\theta)) + \tfrac{15}{64} (a/r)^4 (63\cos^5(\theta) - 70\cos^3(\theta) + 15\cos(\theta))\} \quad (7a)$$

$$B_\theta = (\pi Ia^2)/(cr^3) \{ \sin(\theta) - \tfrac{9}{8} (a/r)^2 (5\sin^3(\theta) - 4\sin(\theta)) + \tfrac{15}{192} (a/r)^4 (315\sin(\theta)(\cos^4(\theta) - 210\sin(\theta)\cos^2(\theta) + 15\sin(\theta))\}, \quad (7b)$$

with an accuracy of 0.05% or better. Hence it is possible to compare the fields predicted by Equations (7) to the observations when the magnetic field of the coils is activated. To do that first we evaluate the factor $(\pi Ia^2)/(cr^3)$, taking into account that 1 Amp (KMS system) = 3 10^9 statamp (Gaussian system), and in Gaussian units the unit of magnetic field B is 1 Gauss = 1 statamp/cm^2,

$$(\pi Ia^2)/(cr^3) = 2.58648\ 10^{-4}\ (0.43464\ 10^{-4}) \text{ Gauss}$$

at the inboard (outboard) magnetometers, with the usual use of fields in nT (1 nT = 10^{-5} Gauss) we obtain a value of

$$(\pi Ia^2)/(cr^3) = 25.8648\ (4.3464) \text{ nT}$$

at the inboard (outboard) magnetometers. Hence we obtain the values for the field

Table '1Mag Dipole'

	B_r [nT]	B_θ[nT]
Inboard ($B_{\_in}$)	17.3451	15.25678
Outboard ($B_{\_ou}$)	3.2658	2.44071

which gives the model $|B_{out}/B_{in}| = 0.1765$. Assuming that for the inboard and outboard magnetometers the sensing axes [Payload system (PL)] are parallel to the spacecraft orthogonal coordinate system, we have the following components for the **B** field:

$$B_{\mathrm{You}} = B_{r\_ou}\, sin(56.48\,^\circ) + B_{\theta\_ou}\, cos(56.48\,^\circ) \qquad (8a)$$

$$B_{\mathrm{Zou}} = B_{r\_ou}\, cos(56.48\,^\circ) - B_{\theta\_ou}\, sin(56.48\,^\circ) \qquad (8b)$$

with the same for the inboard components B_{Yin} and B_{Zin} using $\theta\_{\mathrm{in}} = 61.93\,^\circ$. The cartesian components are given in Table 6 below.

Table '2Mag Dipole'.

	B_{X} [nT]	B_{Y} [nT]	B_{Z} [nT]
Inboard ($B_{\_in}$)	0	+ 22.477	– 5.328
Outboard ($B_{\_ou}$)	0	+ 4.071	– 0.231

These values may be compared to the values observed in X-Y-Z PL coordinate system, in Voyager 2, before the Nov 2006 overheating of the outboard detectors

B_{Xin} = + 0.2 nT; B_{Yin} = 23.912 nT; B_{Zin} = – 4.40 nT, and

B_{Xou} = + 0.010 nT; B_{You} = 4.140 nT; B_{Zou} = – 0.220 nT.

For the sake of a simple expression we use the standard polar representation of the dipole magnetic field generated by the coil at the location of each magnetometer. Notice the addition of higher terms in the dipole expansion, due to the comparable dimension of the coil with the distance of the magnetic sensors to the center of the coil. The transformation from the PL coordinates to the magnetic dipole field of the coil in spherical coordinates is the following:

Table '3Mag Dipole': The expansion dipole field contributions at in/out-board distances at $r_{\mathrm{in}}/r_{\mathrm{ou}}$, θ_{in}, θ_{ou}

Index n	Inboard coeff.		Outboard coeff.	
	$a(r_{I\,n}, n)$	$a(\theta_{in}, n)$	$a(r_{ou}, n)$	$a(\theta_{ou}, n)$
0	– 0.93894	– 0.88295	– 1.10446	– 0.83369
1	– 0.08140	– 0.00620	– 0.02270	– 0.00910
2	+ 0.01500	+ 0.00410	+ 0.000068	+ 0.00044
3	– 0.00057	+ 0.00025	– 0.000004	+ 0.00003

Hence

B_{r_in} = 25.8648 $\Sigma_{\mathrm{n}}\, a(r_{I\,n}, n)$ nT = – 26.01766 nT
B_{θ_in} = 25.8648 $\Sigma_{\mathrm{n}}\, a(\theta_{in}, n)$ nT = – 22.885175 nT
B_{r_ou} = 4.3464 $\Sigma_{\mathrm{n}}\, a(r_{ou}, n)$ nT = – 4.8988 nT
B_{θ_ou} = 4.3464 $\Sigma_{\mathrm{n}}\, a(\theta_{ou}, n)$ nT = – 3.66106 nT

Then |Boutboard/Binboard| = 0.1765.

Appendix **Method**.

The determination of the value of the magnetic field sensed at each orthogonal direction of the *inboard* and *outboard* magnetometers starts with the inspection of each sensor signal to identify possible jumps which are not observed in both magnetometers (*inboard* and *outboard*). This is part of our defined *dual technique* in the estimation of the ambient magnetic field. Then this information is combined with the measurement of the zero-fields in the X-Y PL plane provided by the rolls value. for the Z PL direction it is assumed that it has a zero mean value over an interval of ~ 50 days, as it is described in Section 4. The combination of these key elements constitutes the starting source of information to the identification of the estimated zero-baseline of the magnetic field, as it is illustrated in the Figure App. **Method** 1.

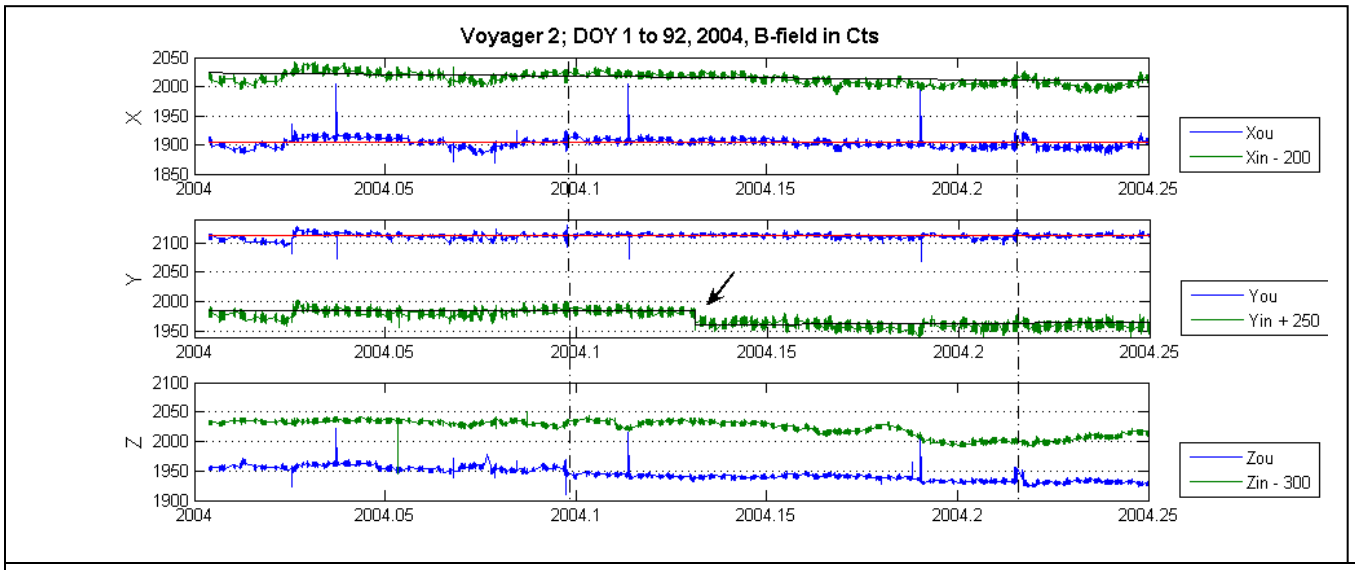

Figure App **Method** 1. Top panel shows the X signal (in Counts) as a function of time (Year): *outboard* with blue line, interpolation between roll values with red, for *inboard* signal with green line and interpolation between rolls in black. Middle panel is same as top panel but for the Y signal. Bottom panel only shows the Z *outboard* and *inboard* signals as in Top.

The vertical dash lines show two consecutive rolls in the interval 2004.01 to 2004.25 in the Figure. The arrow shows a sudden change in signal only in the *inboard* magnetometer Y PL direction. It is possible to use lines to interpolate between the rolls for a first estimate of the zeroes for Xou, in, and You. For Yin we must considerate the *'spurious'* jump in the Yin signal (central panel arrow pointing at approximately 2004.13). The figure also shows a *slow* signal drift for Zin, between 2004.15 and end of the interval. We base this interpretation in the abscense of such signal in the *outboard* corresponding sensor (blue curve, bottom panel). There is the slow drift for the Zin signal, as well as the ones outlined more clearly for Xin, Xou from the drawing of the corresponding lines connecting zero determinations at rolls near 2004.1 (DOY 035) and 2004.21 (DOY 078). The bottom panel also shows the presence in Zou, at rolls, of a spurious wave of period comparable to the data collection time interval (from ~ 4 to 12 hours), and often of ~ 20 Cts amplitude. This spurious 'wave' appears simultaneously with a reduced intensity in the Xou signal.

In the three panels of the figure, the vertically aligned outboard outliers (blue lines), approximately 29 days apart, indicate the times of the MAGCALs (see Section 3). Other smaller outliers are also present in the data, as the figure illustrates. In many cases it is difficult to distinguish between 'outliers' and the signal.

The figure App **Method** 1, also shows more intense *noise* (with a variable amplitude smaller than ~ 4 Cts) in the *inboard* than in the *outboard* signal (green lines). Those noisier *inboard* signals were first identified for the Voyager 2 Xin to have a period of 12.8 min (~ 768 s, i.,e., a frequency of 0.0013020833 s^{-1}). A less steady but similar if not equal spurious 768 s wave(s) is also present the B_{Yin} signal as well as in the Voyager 1 the B_{Xin} and B_{Yin} signals. An example of the partially subtracted spurious activity clustered around a ~ 768 sec period wave in the data set with a sampling every 48 sec is illustrated in the Figure App **Method** 2.

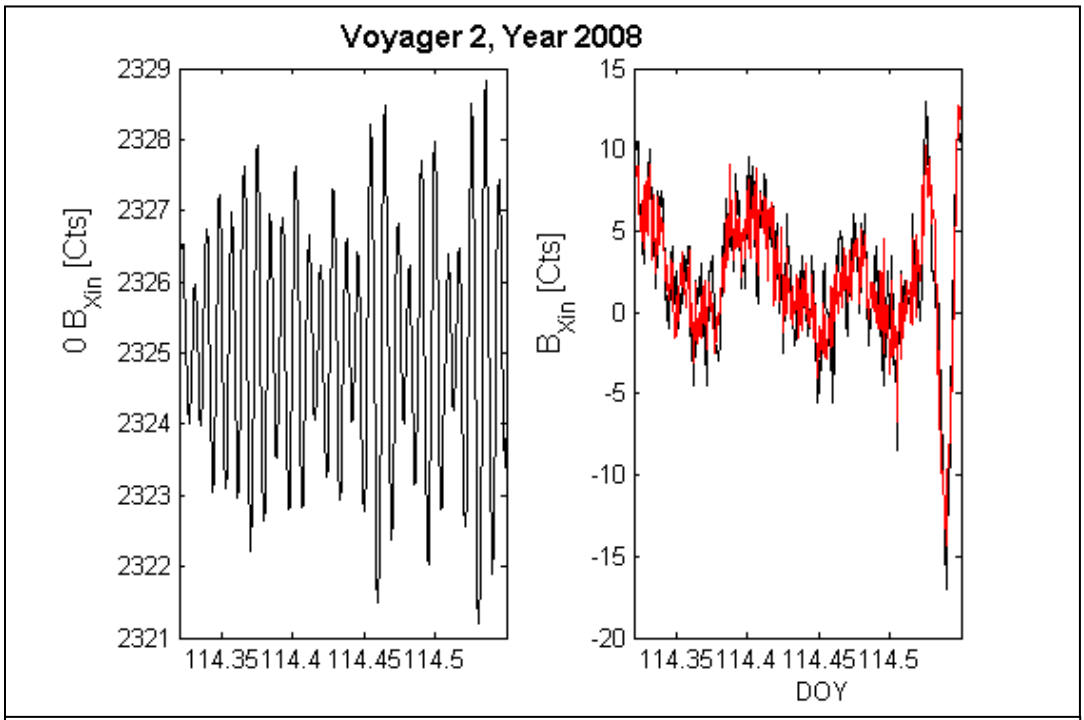

Figure App **Method** 2. Left panel shows estimated ambient field for the X *inboard* signal as a function of time (DOY). Right panel shows the ambient estimated field signal (X *inboard*) without (black) and with (red) correction of the spurious wave signal present in the X *inboard* data.

For the Voyager 2 roll shown in Section 5, the Figure App **Method** 2 shows on the left the amplitude of the ~ 12.8 min period oscillation present in the data. In the right panel of the figure we see the improved magnetic field signal with the spurious range of frequency filtered out (red curve).

Another major source of perturbations to the signal is the presence of 'long- and variable-period disturbances', also pointed out in Figure App **Method** 1 characterized by the presence of a low, variable period frequency (>30 min), and large amplitude field distortion (wave?) in the Voyager 2 Xou, Zou signals. This disturbance often appears to be triggered at/near the time a roll of the spacecraft starts. In some cases these waves stop at the following spacecraft roll, after several weeks of large amplitude disturbance of the signal. The amplitude of the disturbance is often larger than the actual magnetic field strength, as the example below illustrates.

Figure App **Method** 3 illustrates a case of *long- and variable-period disturbances* (waves?) in the Zou sensors signal which started at the roll at 2004.327 (DOY 119) and ended at the roll at 2004.467 (DOY 170) (indicated with vertical black solid lines in the Figure). By correcting for the disturbances we identify the overall trend as observed in *inboard* and *outboard* magnetometers. We assume that the most accurate

representation of the ambient magnetic field signal is the one showing less variation in its local or long time trend(s).

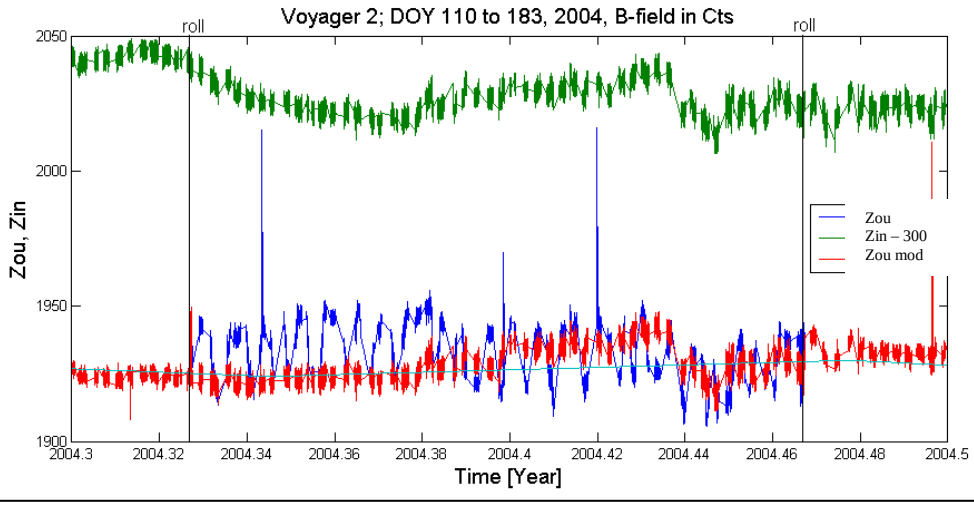

Figure App **Method** 3. Figure shows the Z *outboard* signal (blue line) in Counts, the Z *inboard* signal (green line), and the Z *outboard* signal (red line) modified after preliminary correction for the long period amplitude 'wave-like' structure.

Keeping these considerations in mind we proceed to remove these *long-amplitude/variable-period disturbances* by the modeling of the outboard Z PL component after the Z *inboard*, smoothed signal, as it is illustrated in the figure below. In this approximation the red curve represents the modified Z *outboard* signal. In this example there are two cases to be considered: a) From 2004.3 to ~ 2004.37 it appears that the long time steady trend, highlighted by the preliminary zero for Zou (the light-blue line), is approximately constant, and b) From ~ 2004.37 to the end of the time interval the *outboard* and *inboard* data signals appear to show the same long term trend. The effects on the data for the whole interval are illustrated with Zou-mod, the orange curve in the figure.

Henceforth, the orange curve in the Figure App **Method** 3 represents a first approximation to the ambient signal in Zou after correcting for the presence of the *long-amplitude/variable-period disturbance* identified between the two consecutive rolls at DOY 119 and 170 on year 2004.

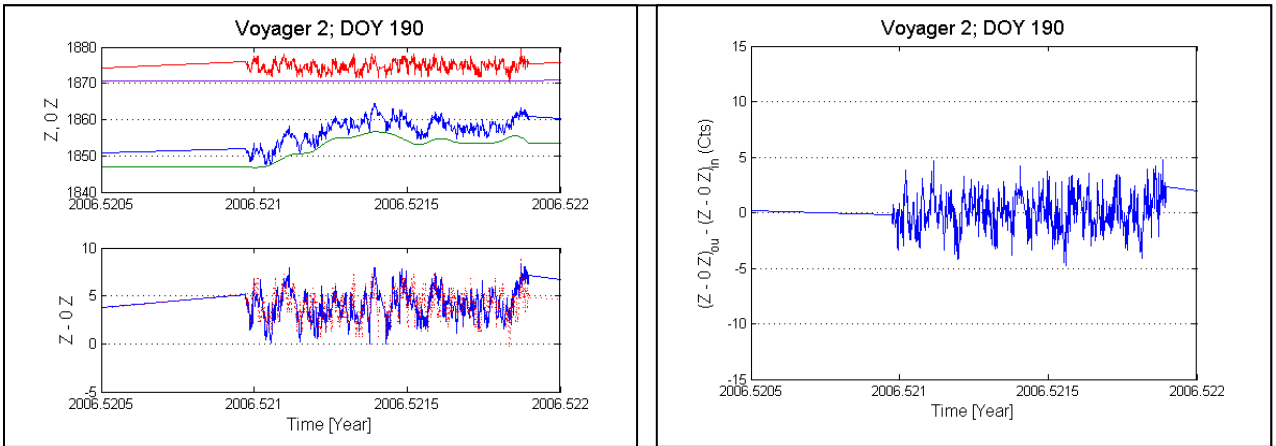

Figure App **Method** 4. The top left panel shows Z *outboard* (blue line) and *inboard* (red line), the estimated *out-board* ambient zero (green line), and the *inboard* zero (violet line) as a function of time (Year). Bottom left shows the resulting estimated field in the Z direction (in Counts) from the *outboard* (blue line) and the *inboard* (red dotted line) for same time interval. On the right panel we plot the residual 'noise' from the Z *outboard* and *inboard* signals.

The signal processed on DOY 190, 2006, shown in the figure above (Figure App **Method** 4) illustrates the presence of *long-amplitude/variable-period disturbance* in the *outboard* sensor of Z-axis detector and its correction (using as a guidance the baseline of the Z-axis sensor in the *inboard* magnetometer).

A consequence of the overheating of the *outboard* detectors in Voyager 2 is a more unstable zero level for each one of the *outboard* magnetometer sensors with variations from one day to another that often reach several sensitivity units (Counts). Because of that effect on the determination of overall magnetic field reference level (ambient zero) for each daily data interval in Voyager 2, we rely most heavily on the *inboard* magnetometer for identifying trends, as illustrated in the figure below.

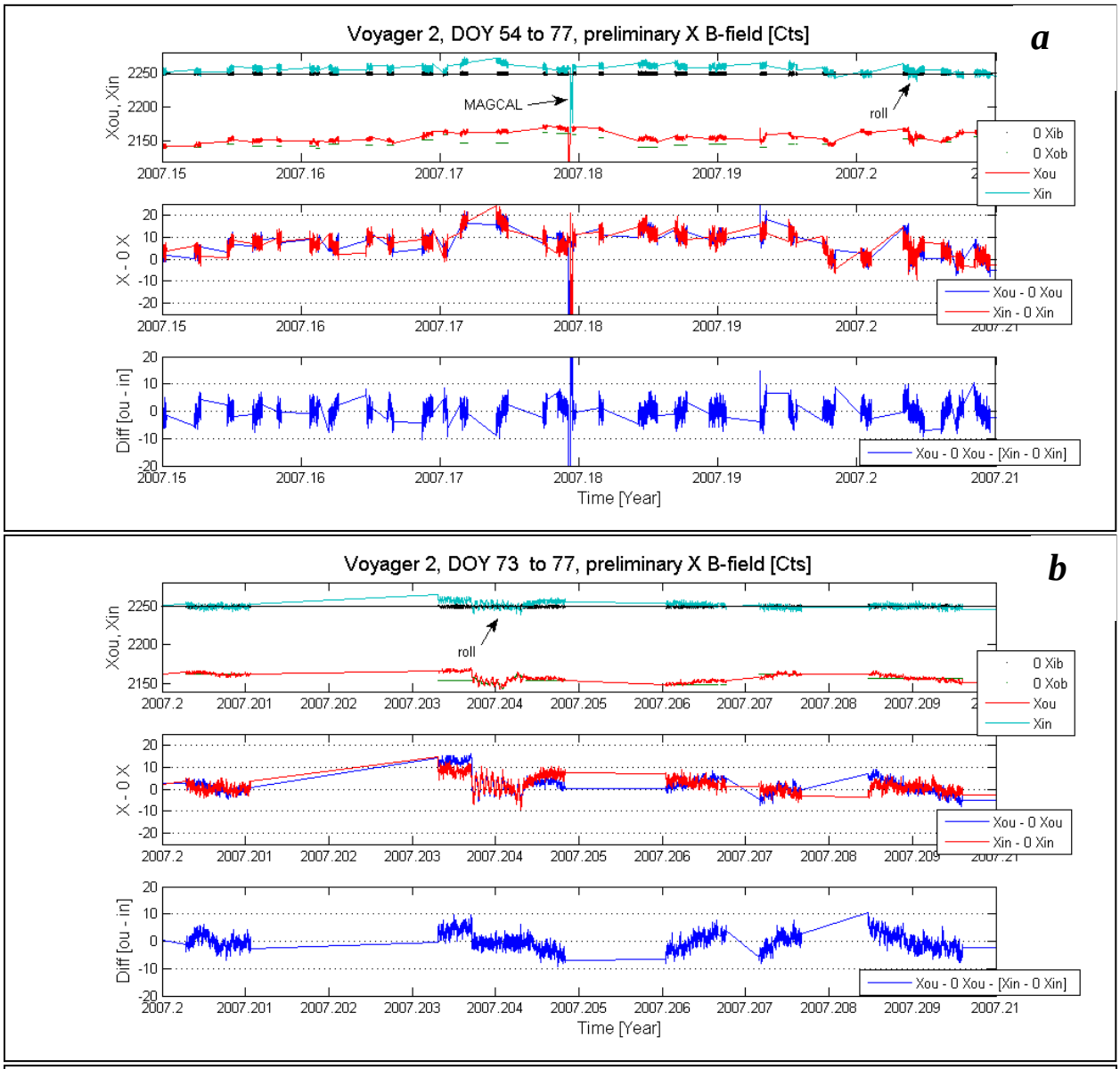

Figure App **Method** 5. **Part *a*** shows in the top (panel 1) a green line corresponding to the X *inboard* signal (Counts) as a function of time (Year), a red line is the X *outboard* signal, a black line is the X *inboard* estimated ambient zero, and a green line, for the X *outboard*. The middle (panel 2) shows the ambient signal from *inboard* (red) and *outboard* (blue) X sensors. The bottom line shows the difference between these preliminary evaluations of the *outboard* and *inboard* X B-field signals. **Part *b*** also shows the signals (detailed view near a roll).

Finally there is the presence of spurious spike like points (and point-like very short intervals). They are often easy to identify by eye, but they are often comparable to or smaller than the points in the signal (Figure App **Method** 5shows spurious points which cannot be eliminated by filters or other standard methods. They must be removed by hand. In Voyager 2 their intermittent and pervasive presence, days in, days out are another challenge to the generation of a clean signal product to be used by the magnetic field expert and even more so for the regular science data user.

The Figure App **Method** 6 shows in the outboard signal along the Y and Z PL directions the presence of spurious dips (top panel) and peaks (bottom panel) in a scale (counts) that is compatible with natural variation of the ambient field signal. These spurious dips and peaks, in this case are present in the averaged field sampled at a rate of one every 48 sec.

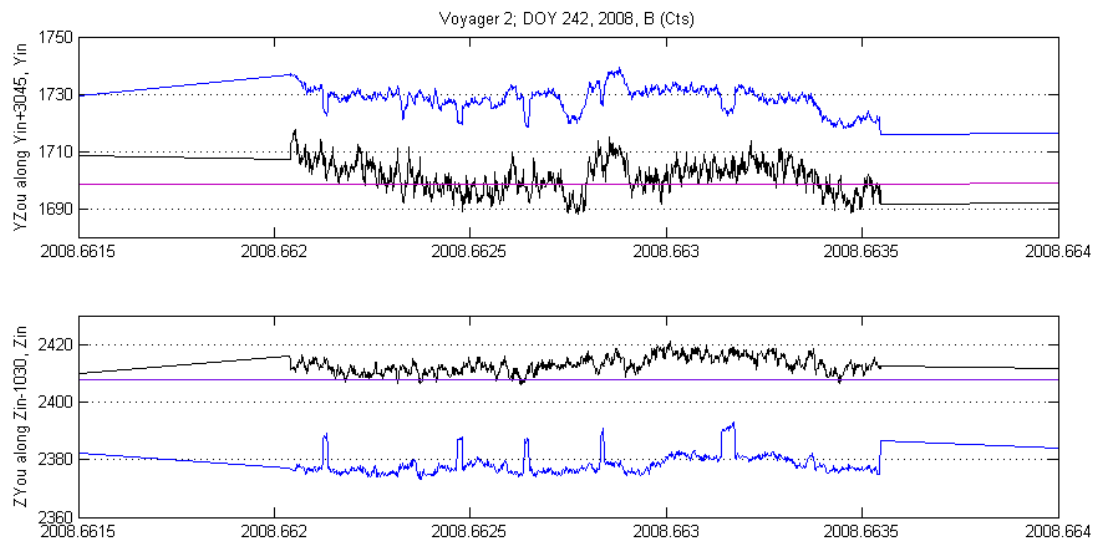

Figure App **Method** 6. The top panel shows with the blue line the Y PL *outboard* signal (in Counts) as a function of time (Year), same for the *inboard* signal (black line) and with the red line the *inboard* estimated ambient zero level. The bottom panel shows the same for the Z PL *inboard* and *outboard* signals as a function of time.

This rather simple example makes it clear that in the same interval (telemetry downlink) we see signals in inboard and outboard sensors which are real and have comparable amplitude and duration to some of the spurious intervals. Two examples of intervals in which the noise points are intermingled with "real" points and cannot be removed by a computer algorithm are shown below (private communication, L.F. Burlaga). There is no simple pattern of the noise (shown by the red points). New forms appear as new data are processed, so that any algorithm that might be developed for known mixtures of noise and signal will generally not apply to new observations. Except for cases of extreme outliers, the noise points must

be identified by detailed examination of all the information available and with some judgment.

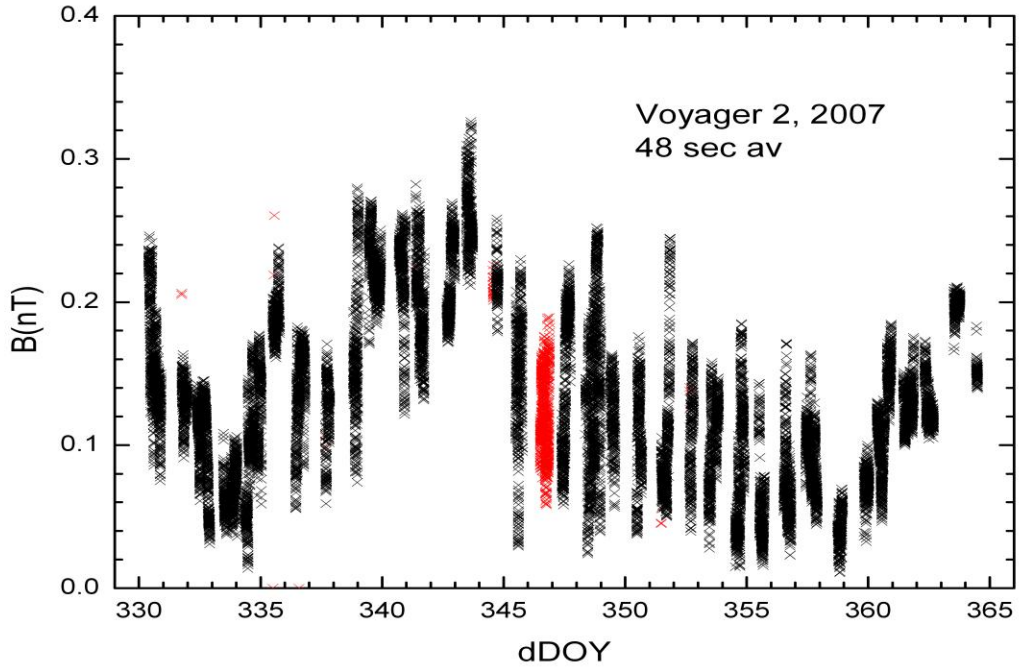

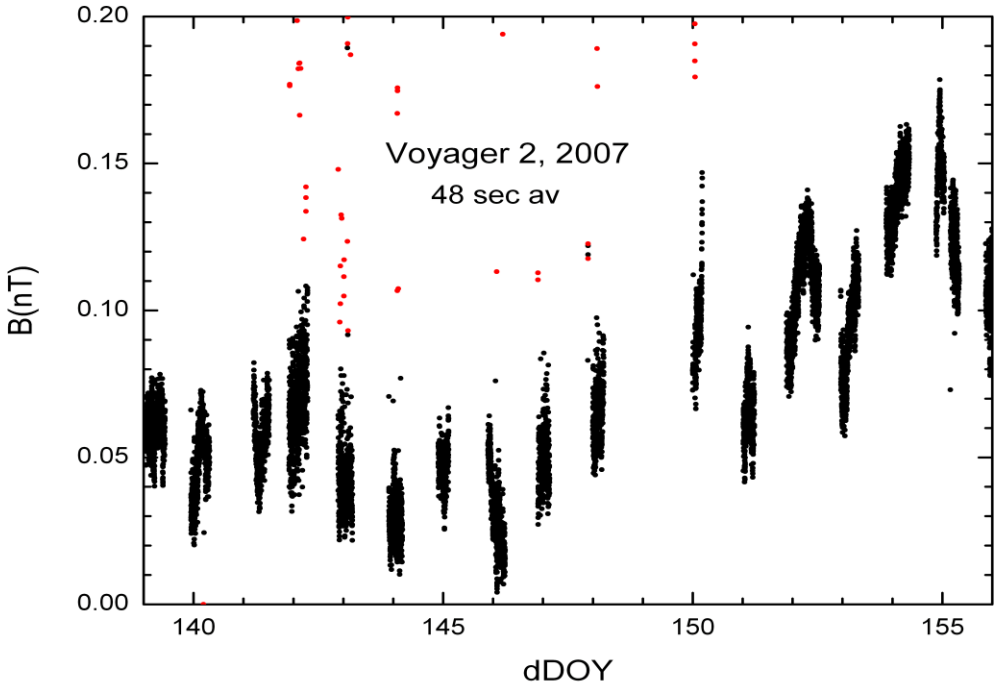

References

1- Aschenbrenner H., and G. Goubau, Hochfreq Tech Electroakust **47**,178, 1936.
2- Space-based magnetometers, Mario H. Acuña, Rev. of Scien. Ins., **73**, pp 3717-3736, 2002.
3- Standard 'spacecraft coordinates' as defined in JPL Document 618-205.
4- by R.P. Lepping, result of interpolation, listed as 'of A19zero2 and A1Azero2., code B19zero2', 1978.
5- Acuña, M. H., Voyager GSFC Magnetic Field Experiment In-Flight sensor Alignment Determination, 1978
6- Burlaga, L.F., Interplanetary Magnetohydrodynamics, 1995.
7- Burlaga L.F., N.F. Ness, M.H. Acuña, R.P. Lepping, J.E.P. Connerney and J.D. Richardson, Magnetic fields at the solar wind termination shock, Nature, **454**|3, pp 75-77, 2008.
8- Jackson, J.D., Classical Electrodynamics,

Behannon, K.W., M.H. Acuña, L.F. Burlaga, R.P. Lepping, N.F. Ness, and F.M. Neubauer, Magnetic-Field Experiment for Voyager-1 and Voyager-2, Space Science Reviews, 21 (3), 235-257, 1977.

Burlaga, L.F., Merged interaction regions and large-scale magnetic field fluctuations during 1991 - Voyager-2 observations, J. Geophys. Res., 99 (A10), 19341-19350, 1994.

Burlaga, L.F., N.F. Ness, Y.-M. Wang, and N.R. Sheeley Jr., Heliospheric magnetic field strength and polarity from 1 to 81 AU during the ascending phase of solar cycle 23, J. Geophys. Res., 107 (A11), 1410, 2002.

Connerney and Kempler, Notes on the Voyager noise problem,1989.

Ness, N., K.W. Behannon, R. Lepping, and K.H. Schatten, J. Geophys. Res., , 76, 3564, 1971.